Factors influencing shallow (< 1000 m depth) temperatures and their significance for extraction of ground-source heat

Trond Slagstad[1], Kirsti Midttømme[1,2], Randi Kalskin Ramstad[1,3] and Dag Slagstad[4]

[1] Geological Survey of Norway (NGU), 7491 Trondheim, Norway.
[2] Norwegian Geotechnical Institute (NGI), Pb. 1230, Pirsenteret, 7462 Trondheim, Norway.
[3] Asplan Viak AS, Pb 6723, 7031 Trondheim, Norway.
[4] SINTEF Fisheries and Aquaculture, 7465 Trondheim, Norway.
E-mail: trond.slagstad@ngu.no

The thermal structure of the shallow crust (defined here as < 1000 m depth) is sensitive to surface effects including geological variation (e.g., radiogenic heat production, terrestrial heat flow, thermal conductivity), terrain effects (e.g., topography, slope orientation), climatic conditions (e.g., palaeoclimatic history, mean annual surface temperatures) and human activity (e.g., farming, urbanisation). A number of quantitative models show that at shallow depths down to a few hundred metres, mean annual surface temperature is the main factor controlling subsurface temperature, whereas geological variation (heat flow, heat production, thermal conductivity) only becomes significant at depths of ca. 1000 m and greater. Ground-source heat for household heating is commonly extracted from shallow boreholes between 100 and 200 m deep; thus, at present, the effects of variation in heat flow and heat production are negligible, whereas thermal conductivity has some impact on the amount of heat that is extractable from the ground. Rather, one should focus on gathering information about thickness of overburden and hydrogeological activity, as well as reducing costs by developing cheaper, more efficient drilling techniques and heat pumps. With technological advances allowing affordable drilling to depths on the order of 1000 m, geological information will become increasingly more important.

Slagstad, T., Midttømme, K., Ramstad, R.K. and Slagstad, D. (2008) Factors influencing shallow (< 1000 m depth) temperatures and their significance for extraction of ground-source heat. *In* Slagstad, T. (ed.) *Geology for Society*, Geological Survey of Norway Special Publication, **11**, pp. 99–109.

Introduction

The thermal structure of the shallow continental crust (taken here as < 1000 m depth) is a function of heat flow from the Earth's interior, geological heterogeneity, surface effects (herein referred to as 'terrain effects', cf., Blackwell et al. 1980), surface temperatures and past climatic changes. The heat flowing from the Earth's interior is dominantly derived from radioactive decay of U, Th and K in the Earth's mantle and crust (Hofmeister and Criss 2005), and shallow geological effects include variation in radiogenic heat production and thermal conductivity, variable soil or till cover and hydrogeological activity. The main terrain effects are topographic relief, microclimatic variations from differences in vegetation cover, and varying solar influx as a function of slope orientation and slope angle (Blackwell et al. 1980). Long-term climatic variation (palaeoclimatic history), particularly in formerly glaciated areas, and mean annual surface temperature are important contributors to the shallow thermal structure (e.g., Clauser et al. 1997), and, in addition, human activity such as farming and urbanisation may locally change the thermal structure of the shallow crust (e.g., Taniguchi and Uemura 2005).

The purpose of this paper is to present generalised models that quantify the shallow thermal effects of some of the parameters mentioned above and discuss these in terms of utilisation of ground-source heat in houses and small buildings. We limit our discussion to variations in shallow radiogenic heat production and thermal conductivity, topographic relief, palaeoclimatic history and mean annual surface temperature—that is, factors related to conductive heat transfer. Convective heat transfer, in particular groundwater flow, is not discussed. The models and conclusions are based on and applicable to extraction of heat from crystalline bedrock in tectonically inactive areas, where conduction through a solid is the only means of heat transfer.

The modelling shows that although geological, terrain and palaeoclimatic factors contribute to the shallow thermal structure, their significance for extraction of ground-source heat is rather minor in the geological settings considered here (e.g., Scandinavia), and the main factor determining temperatures at shallow depths is the mean annual surface temperature.

Factors influencing shallow crustal temperature and heat flow

Below, we present 1D, 2D and 3D thermal models that address the geological, terrain and palaeoclimatic effects mentioned above. Ground-source heat is typically extracted from boreholes that are between 100 and 200 m deep; however, in the foreseeable future, drilling to 1000 m or deeper may become economically feasible. We therefore present modelled temperature and heat-flow data from depths of 100, 200 and 1000 m in the models and base our discussion on these. The models were developed and run using the Comsol Multiphysics finite element method software (COMSOL AB Sweden, COMSOL Multiphysics v. 3.3a).

Radiogenic heat production

Variation in radiogenic heat production causes variation in heat flow and thus thermal gradient. These factors can be addressed by simple 1D calculations assuming a given, constant surface temperature (T_{sur}, °C), basal heat flux (Q_0, mW m^{-2}) and thermal conductivity (k, W m^{-1} K^{-1}), and varying radiogenic heat production (A, μW m^{-3}) or thickness of the heat producing layer (h, km) (Figure 1a). The steady-state heat flow (Q) and temperature (T) at depth (z, km), where z is positive upwards, can be derived from Fourier's law of heat conduction, slightly modified to also include internal heat sources (1):

$$-k\frac{dT}{dz} = Q_0 + A(z+h) \qquad (1)$$

as

$$Q(z) = A(z+h) + Q_0 \qquad (2)$$

and

$$T(z) = T_{sur} - \frac{Q_0}{k}z - \frac{A}{2k}z^2 - \frac{A}{k}hz \qquad (3)$$

In Norway, typical surface heat-flow (Q_{sur}) values range between 40 and 60 mW m^{-2}, but locally exceed 70 mW m^{-2} in areas underlain by thick, high heat-producing granites (e.g., Grønlie et al. 1977, Heier and Grønlie 1977, see also discussion in Slagstad 2006). One such granite is the Iddefjord–Bohus granite in southeast Norway and southwest Sweden that ranges in thickness between ca. 1 and 5 km (Ramberg and Smithson 1973, Landström et al. 1980, Lind 1982), with an average heat-production rate of ca. 6 μW m^{-3} (Slagstad 2006, Slagstad in press). Here, we present the results of 1D calculations that quantify the thermal effects of a high heat-producing layer, like the Iddefjord–Bohus granite, ranging in thickness from 0 to 5 km with a heat production of 6 μW m^{-3}, corresponding to a 30 mW m^{-2} variation in surface heat flow. The top of the high heat-producing layer is kept at the surface, the surface temperature is constant at 0°C, and the basal heat flow is constant at 40 mW m^{-2}. The model geometry and parameters are shown in Figure 1a. Figures 1b and 1c show temperature and heat-flow anomalies, respectively, at 100, 200 and 1000 m depth as a function of the thickness of the high heat-producing layer. The temperature and heat-flow anomalies are calculated relative to the thermal structure of a similar model without a high heat-producing layer (i.e., h = 0).

At 100 and 200 m depth, the thermal anomaly imposed by a 5 km-thick, high heat-producing (6 μW m^{-3}) layer is 1 and 2°C, respectively. This temperature anomaly corresponds to a 30 mW m^{-2} increase in surface heat flow, which probably represents a maximum in terms of the variation one might expect in

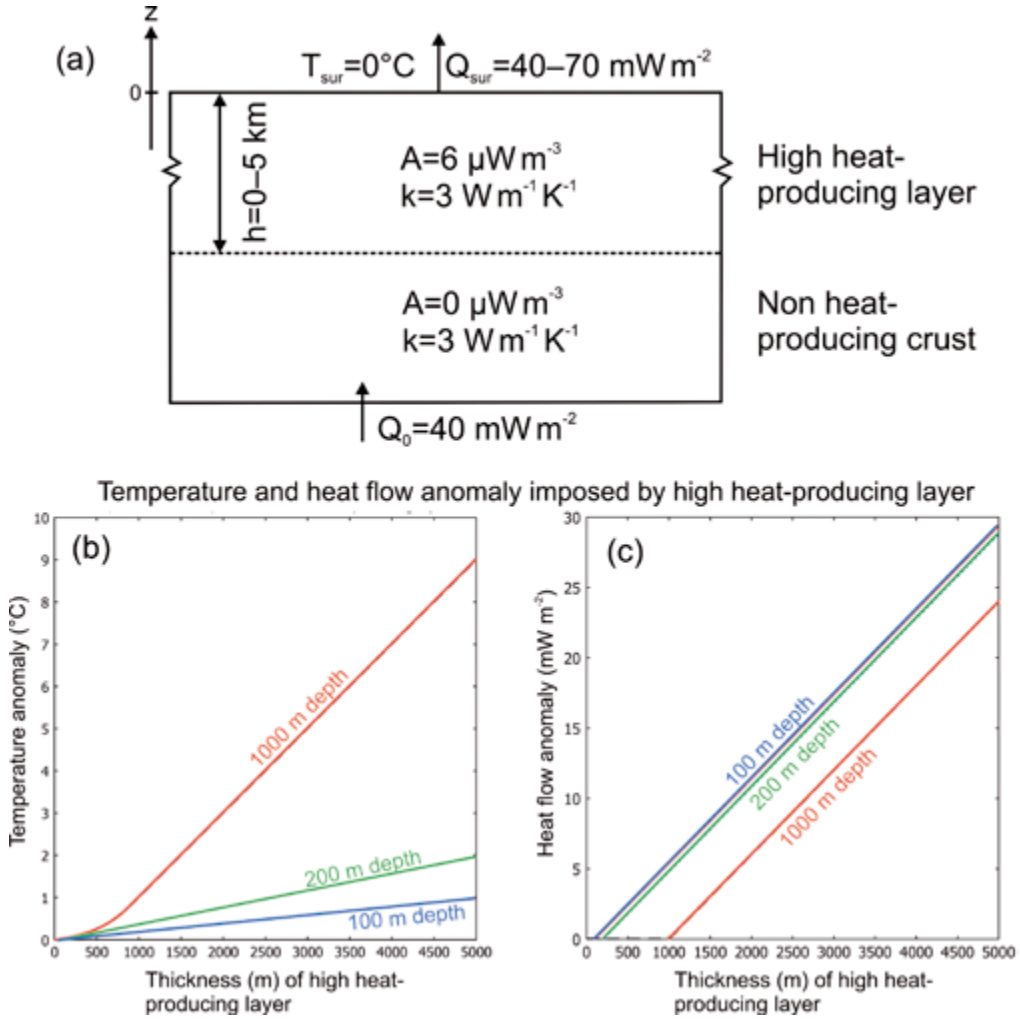

Figure 1. (a) Model geometry and input parameters of a model investigating the significance of heat production on the near-surface thermal structure. (b) and (c) Temperature and heat flow anomalies, respectively, at 100, 200 and 1000 m depth, imposed by a high heat-producing layer, for example certain granite bodies, at the surface.

geologically stable areas. The results of the modelling thus show that the temperature in the uppermost few hundred metres is relatively insensitive to variations in heat production (and heat flow). At 1000 m depth, the thermal anomaly is 9°C for a 5 km-thick high heat-producing layer. The heat-flow anomaly increases linearly with increasing thickness of the heat-producing layer, reaching nearly 30 mW m^{-2} at 100 and 200 m depth when the layer is 5 km thick. At 1000 m depth, the anomaly is obviously smaller, but nevertheless significant, reaching nearly 25 mW m^{-2} for a 5 km-thick, high heat-producing layer.

Thermal conductivity and low-conductivity overburden

In contrast to variation in radiogenic heat production, variation in thermal conductivity only affects the thermal gradient but not the heat flow. Given no internal heat production (i.e., $Q_{sur} = Q_0$), Equation (3) can be reduced such that the temperature at a certain depth is expressed as:

$$T(z) = T_{sur} - \frac{Q_0}{k} z \qquad (4)$$

Here, we consider the thermal effects of conductivities varying between 2 and 4 W m^{-1} K^{-1}, which covers most rock types encountered in the continental crust (Clauser and Huenges 1995). Figure 2a shows how the temperature at 100, 200 and 1000 m depth varies with varying thermal conductivity given surface heat flows of 40, 50, 60 and 70 mW m^{-2}. Because thermal gradient is inversely related to thermal conductivity, the temperature effect is proportional with increasing depth. This inverse relationship also means that temperatures at a particular depth converge with increasing conductivity. Thus, at 100 m depth, variation in thermal conductivity from 2 to 4 W m^{-1} K^{-1} and surface heat flow between 40 and 70 mW m^{-2} amounts to ca. 2.5°C variation in temperature; at 200 m depth the corresponding value is ca. 5°C, and at 1000 m is ca. 25°C. Figure 2b shows calculated temperature anomalies relative to a model with thermal conductivity 3 W m^{-1} K^{-1}. For shallow depths (100 and 200 m), the temperature anomalies are small, on the order of 2 to 3°C, despite the relatively large variation in conductivity. At greater depths (1000 m), the temperature anomalies are naturally larger, on the order of 10–20°C. The temperature effects imposed by variations in conductivity are thus slightly higher than for variations in radiogenic heat production; however, at the shallow depths from which ground-source heat is normally extracted, the variation is at most a

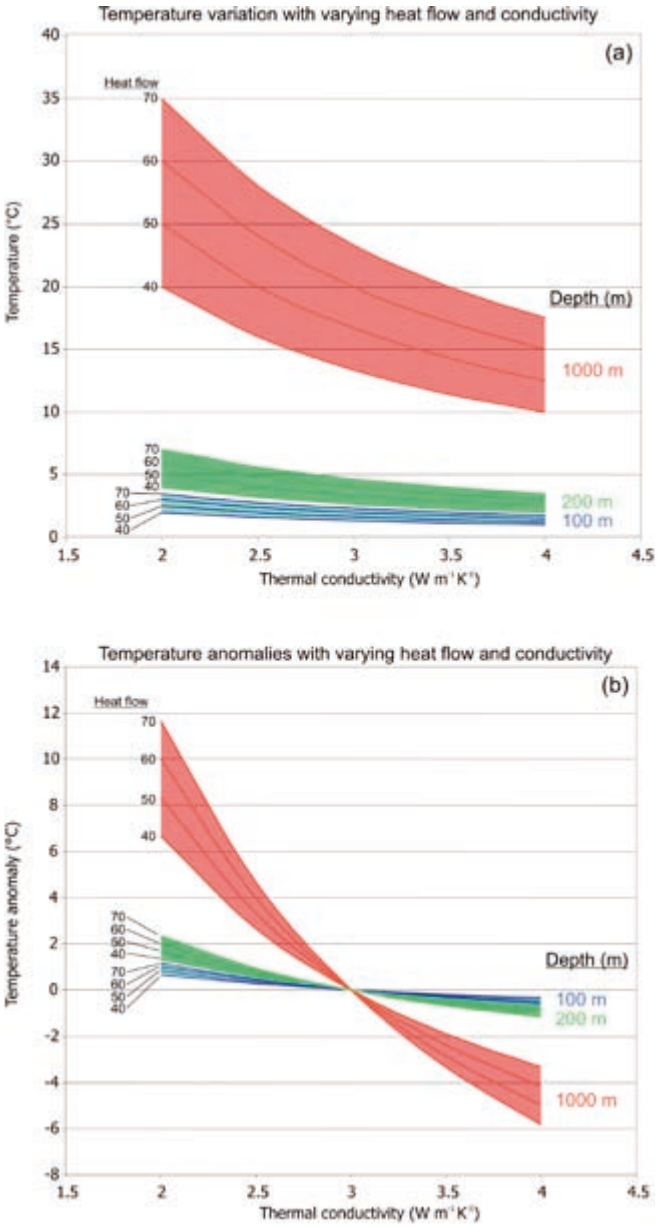

Figure 2. (a) Temperatures at 100, 200 and 1000 m depth with varying thermal conductivity given surface heat flows of 40, 50, 60 and 70 mW m^{-2} and a surface temperature of 0°C. (b) Thermal anomalies calculated relative to a model with conductivity 3 W m^{-1} K^{-1}, otherwise similar to (a).

few degrees, even when considering rather large variations in conductivity and heat flow. A downside is that the higher subsurface temperatures are attained at low conductivities that in turn reduce the amount of heat that is extractable from the ground (discussed further below).

Another factor related to thermal conductivity is the presence of overburden such as sand, clay and moraine. Such materials typically have thermal conductivities that are far lower than most rock types (Midttømme 1997), thereby acting as low-conductivity thermal blankets that will increase the subsurface temperature. In a two-layer model with overburden as the upper layer and bedrock as the lower layer, elevated temperatures attained due to high thermal gradients in the upper, low-conductivity layer will propagate down through the lower layer. In most cases, thick accumulations of overburden are located in valleys, in which case lateral heat flow will limit the blanketing effect to rather shallow depths of a few hundred metres. The thermal effects of such a low-conductivity layer can easily be assessed by considering Equation (4), which, being a 1D equation, represents a maximum estimate of these effects by neglecting lateral heat flow.

Figure 3a shows temperature anomalies resulting from overburden of variable thickness (10, 50 and 100 m) as a function of thermal conductivity (0.5–1.5 W m^{-1} K^{-1}) and heat flow (40–70 mW m^{-2}). The anomalies are calculated by

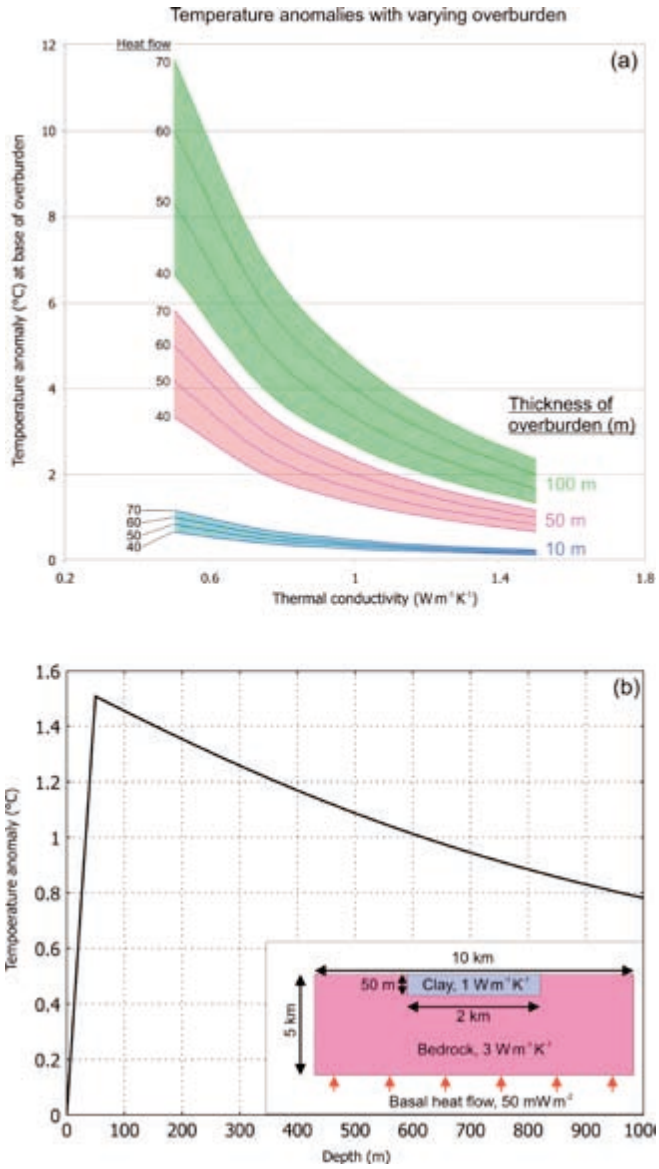

Figure 3. (a) Temperature anomalies at base of 10, 50 and 100 m-thick low-conductivity layers consisting of clay or other types of unconsolidated overburden for various heat flows and thermal conductivities. The temperature anomalies are calculated relative to the temperatures at 10, 50 and 100 m in bedrock with a thermal conductivity of 3 W m^{-1} K^{-1}. (b) Temperature anomaly imposed by a 2 km-wide and 50 m-thick low-conductivity layer (1 W m^{-1} K^{-1}) as a function of depth, given a heat flow of 50 mW m^{-2}. The inset shows the model setup (not to scale).

comparing the temperature at 10, 50 and 100 m depth (i.e., at the base of the low-conductivity layer) with the temperature at the same depth in exposed bedrock with a thermal conductivity of 3 W m^{-1} K^{-1}. The depth of penetration of the thermal anomaly depends on the areal extent of the low-conductivity layer and distance to exposed bedrock acting as conduits for excess heat, but will even for relatively moderate extents of a few kilometres and thickness of a few tens of metres, penetrate to depths of several hundred metres. This is illustrated by the 2D model in Figure 3b, which shows temperature anomaly in the horizontal centre of the model as a function of depth imposed by a 2 km-wide and 50 m-thick low-conductivity layer (1 W m^{-1} K^{-1}) given a heat flow of 50 mW m^{-2}. The maximum anomaly at the base of the layer is slightly lower (0.2°C) than predicted from Figure 3a due to lateral heat flow, and tapers off with increasing depth. The modelling shows that very thick low-conductivity layers (at least 50 to 100 m) or with unrealistically low thermal conductivities are required to produce temperature anomalies of a few degrees. Although thick overburden has some impact on temperatures in the shallow crust, overburden requires that the borehole be cased, resulting in inflated drilling costs and discouraging the extraction of ground-source heat.

Topography

The most obvious topographic effects on subsurface temperatures are compressed isotherms (i.e., enhanced gradient) beneath topographic lows (referred to here as valleys), and drawn out isotherms (i.e., reduced gradient) beneath topographic highs (peaks). This relationship is illustrated in Figure 4, which shows temperature and heat flow in a 2D model with a sinusoidal topography with wavelength 10 km and amplitude 1000 m. The temperature at the model surface is 5°C at the valley floor and decreases upward by 6.5°C km^{-1}, equal to the atmosphere's lapse rate. The heat flow at the base of the model is 50 mW m^{-2}, and the model has an isotropic conductivity of 3 W m^{-1} K^{-1}. The discussion on topographic effects below is based on this model.

Figures 5 and 6 show how modelled heat-flow and temperature anomalies (i.e., relative to a horizontal surface), respectively, at 100, 200 and 1000 m depth vary with amplitude (0–1500 m) and wavelength (3–15 km). The plots show that temperature and heat flow are reduced beneath peaks and increased beneath valleys, and that the topographic effect increases with increasing amplitude and decreasing wavelength (cf., Blackwell et al. 1980). Topography clearly has a significant effect on heat flow in the shallow crust, increasing or decreasing heat flow locally by up to several tens of mW m^{-2}. In contrast, temperatures at shallow depths (100 and 200 m) in areas with moderate topography are only weakly perturbed, whereas temperatures at greater depths are more strongly affected. This is analogous to the discussion above on the effect of variation in heat production, which can also be thought of as variation in heat flow: at shallow depths, even relatively large changes in heat flow, and thus thermal gradient, do not result in significant variation in temperature (this also follows from Equation 4). In

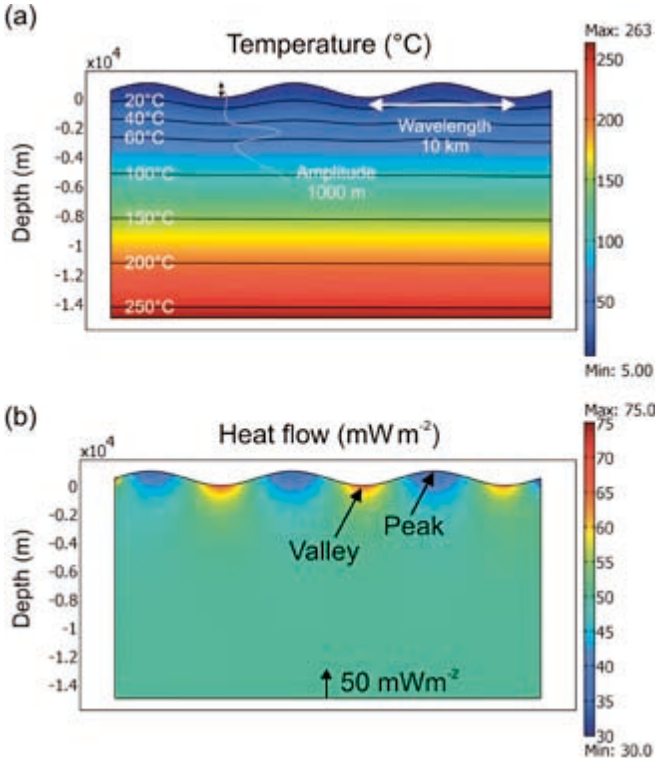

Figure 4. Thermal model illustrating how temperature (a) and heat flow (b) are affected by topography. The thermal parameters are: 5°C surface temperature, 50 mW m^{-2} basal heat flow, a conductivity of 3 W m^{-1} K^{-1}, and no internal heat production.

fact, the magnitudes of heat-flow and temperature anomalies relating to variation in heat production and topography are similar (cf., Figures 1, 5 and 6).

A perhaps surprising feature of the plots in Figures 5 and 6 is the fact that several of the lines for heat-flow and temperature anomalies at 1000 m depth cross each other. This may at first appear counter-intuitive, however, the reason this happens is that for a given wavelength, a point is reached where increasing the amplitude does not affect the subsurface thermal structure noticeably; this point is reached at greater amplitudes for greater wavelengths and/or shallower depths, hence the crossing lines. If the plots had been extended to greater amplitudes, similar effects would appear in the 100 and 200 m plots. Another way of looking at this is that as the walls of the peak–valley topography approach vertical (i.e., very high amplitude), the heat flow and temperature at a given depth will not change in response to further increases in amplitude, apart from the effect of the atmosphere's lapse rate. This relationship is illustrated and explained schematically in Figure 7.

Palaeoclimatic history

The effects of palaeoclimatic changes on subsurface temperature were recognised a long time ago (Anderson 1934, Benfield 1939). Each temperature perturbation at the surface propagates into the subsurface at a rate determined by the diffusivity of the rock, and the depth of penetration depends on both the amplitude and duration of the perturbation at the surface.

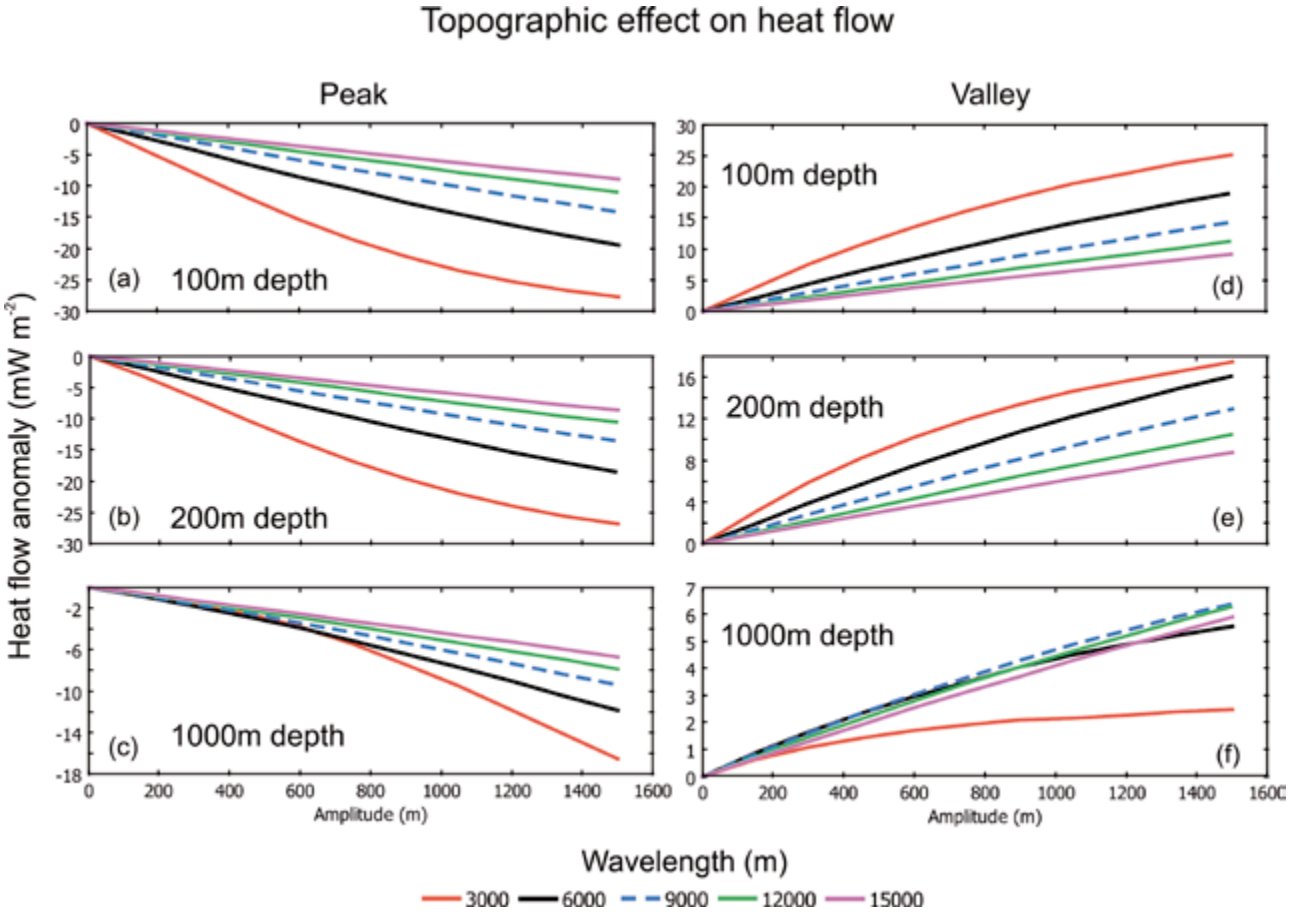
Topographic effect on heat flow
Peak
Valley
Heat flow anomaly (mW m-2)
(a) 100m depth
(b) 200m depth
(c) 1000m depth
100m depth
200m depth
1000m depth
(d)
(e)
(f)
Amplitude (m)
Wavelength (m)
3000
6000
9000
12000
15000

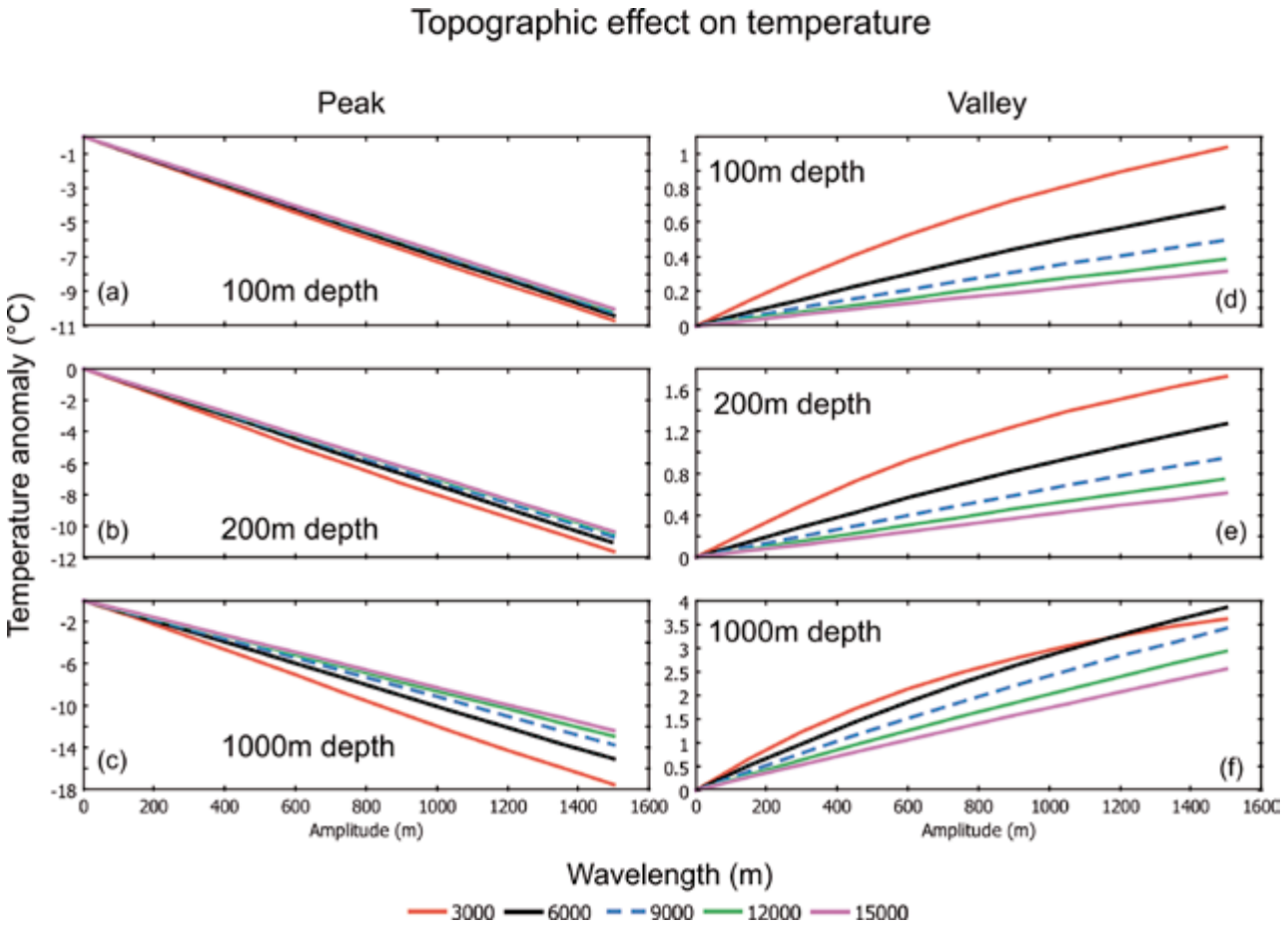
Topographic effect on temperature
Peak
Valley
Temperature anomaly (°C)
(a) 100m depth
(b) 200m depth
(c) 1000m depth
100m depth
200m depth
1000m depth
(d)
(e)
(f)
Amplitude (m)
Wavelength (m)
3000
6000
9000
12000
15000

Figure 5. Influence of topography on heat flow at 100, 200 and 1000 m depth beneath a peak (a–c) and a valley (d–f). The heat-flow anomaly is calculated by subtracting the heat flow at a particular depth given a horizontal surface from the modelled heat flow at the same depth given a sinusoidal topography with a certain wavelength and amplitude. The amplitude varies between 0 and 1500 m, and the wavelength between 3 and 15 km. Thermal parameters as in Figure 4.

Roughly speaking, the effects of Pleistocene ice ages, which lasted several hundred thousand years, extend to depths of several kilometres, climatic changes during the Holocene extend to depths of several hundred metres to a few kilometres, and seasonal changes extend to depths of a few tens of metres. The amplitude of the perturbation varies inversely with the elapsed time since the perturbation, which means that the amplitude of a Holocene perturbation will be greater than the amplitude of a similar-magnitude Pleistocene event.

In order to assess the thermal significance of palaeoclimatic history we have calculated heat-flow and temperature effects at 100, 200 and 1000 m depth for three simple palaeoclimatic histories (Figure 8a): a 'cold' model in which the temperature is constant at -15°C between 30 and 20 ka, followed by a gradual warming to a present-day temperature of 5°C; a 'warm' model where the temperature is -1°C between 30 and 20 ka, followed by a gradual warming to a present-day temperature of 5°C; and a 'tepid' model which is similar to the 'cold' model except that the surface temperature rises to 5°C at 1 ka and remains at that temperature until the present day. The 'cold' model represents periglacial areas or areas beneath cold-based ice, whereas the 'warm' model represents areas beneath warm-based ice. The 'tepid' model is included to assess the rate of thermal recovery after a period of cold climatic conditions.

The modelling is based on a 2D model where temperature at the surface varies as a function of time and temperatures at depth are calculated by solving the time-dependent heat equation (5) using the finite element method.

$$\rho C_p \frac{\partial T}{\partial t} - \nabla(k\nabla T) = Q \qquad (5)$$

where ρ is density, C_p is heat capacity and t is time. Thermal parameters are given in the caption to Figure 8.

Figure 8b shows the heat-flow anomalies (i.e., relative to steady-state conditions) at various depths at the end of the different palaeoclimatic histories (i.e., at present time). The anomaly imposed by the 'cold' model is as high as -50 mW m^{-2} at 100 m depth, and decreases quite rapidly with increasing depth. The 'warm' model produces heat-flow anomalies up to -20 mW m^{-2}, whereas the 'tepid' model is intermediate between the two. Temperatures (Figure 8c) are similarly affected; the 'cold' model produces temperature anomalies of -2 and -3.5°C at 100 and 200 m depth, respectively, and as much as -7°C at 1000 m depth, whereas the 'warm' model yields temperature anomalies of -0.5, -1 and -2°C at 100, 200 and 1000 m depth, respectively. The 'tepid' model again yields intermediate results, with temperature anomalies of -1, -1.5 and -5°C at 100, 200 and 1000 m depth, respectively. These results show that the temperature effect of various palaeoclimatic histories can linger for a long time, particularly at depths greater than several

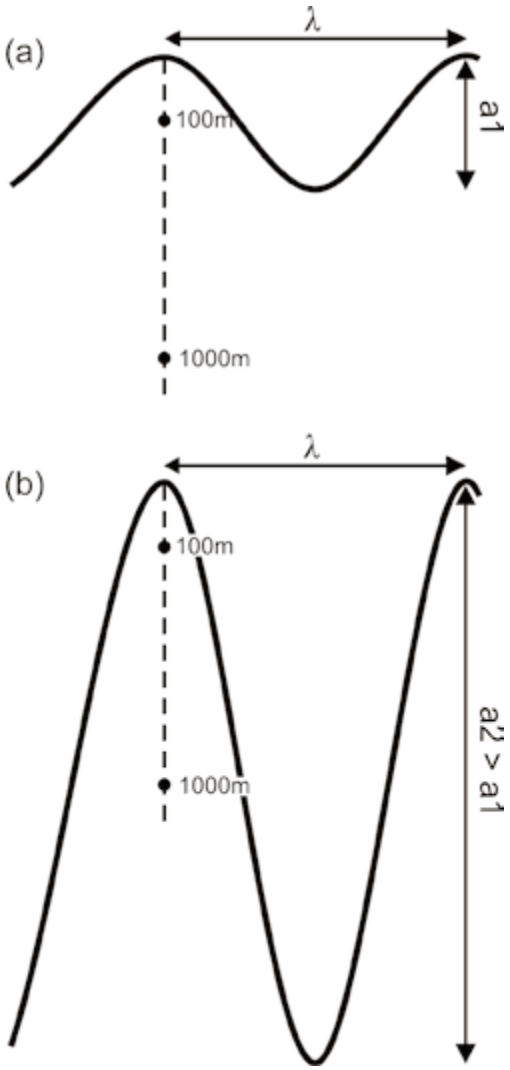

Figure 7. Illustration showing the relative topographic effect at 100 and 1000 m depth of varying amplitude (a1 to a2) for a constant wavelength (λ). (a) Topography with comparatively low amplitude (a1), in which the topographic effect is relatively large at 100 m depth and significantly smaller at 1000 m depth. In (b) the wavelength is the same as in (a) but the amplitude is increased to (a2 > a1). In this case, topographic effects are significant at both depths, however, the relative increase in the topographic effect from (a) to (b) will be greater at 1000 m depth than at 100 m depth.

Figure 6. Influence of topography on temperatures at 100, 200 and 1000 m depth beneath a peak (a–c) and a valley (d–f). The temperature anomaly is calculated by subtracting the temperature at a particular depth given a horizontal surface from the modelled temperature at the same depth given a sinusoidal topography with a certain wavelength and amplitude. The amplitude varies between 0 and 1500 m, and the wavelength between 3 and 15 km. Thermal parameters as in Figure 4.

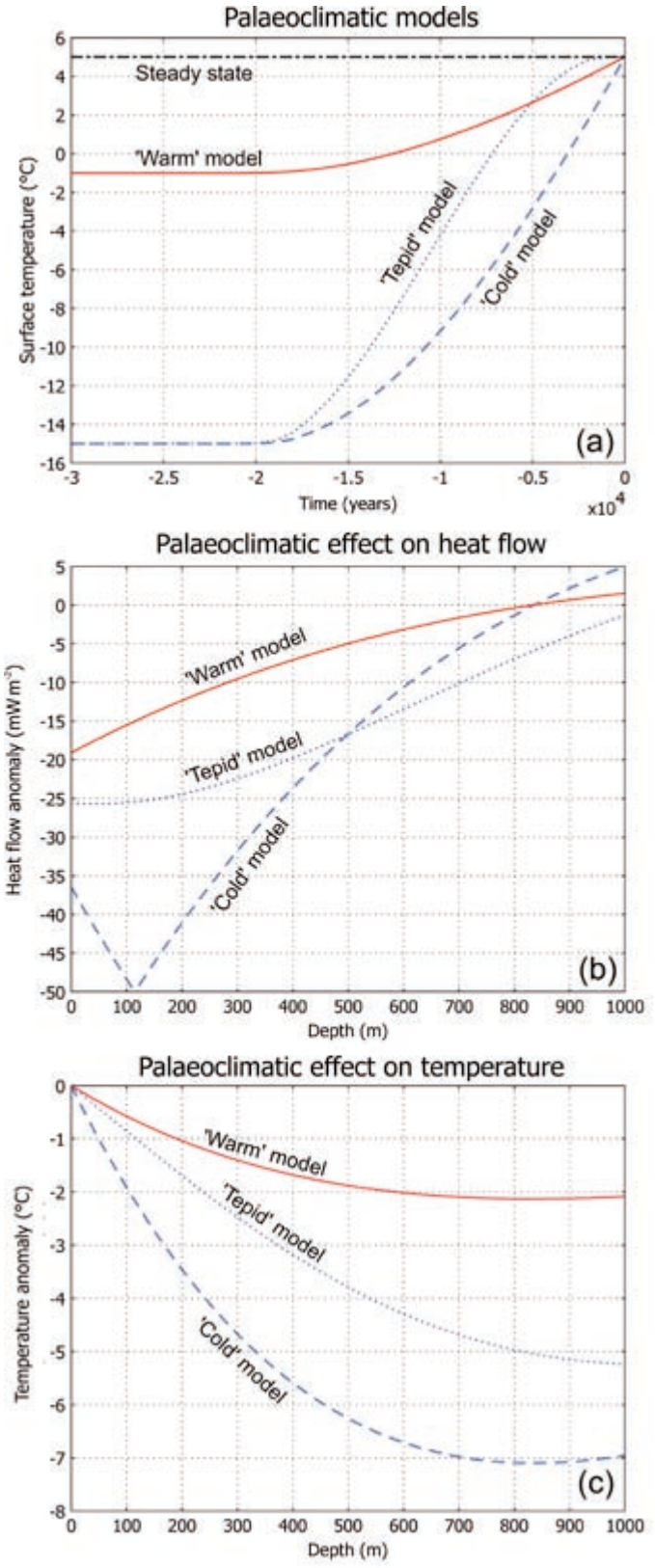

Figure 8. (a) Modelled 'warm', 'tepid' and 'cold' palaeoclimatic histories. The modelling assumes a constant heat flow of 50 mW m^{-2}, thermal conductivity of 3 W m^{-1} K^{-1}, heat capacity of 850 J kg^{-1} K^{-1} and density of 2800 kg m^{-3}. The initial (i.e., prior to 30 ka) steady-state thermal conditions of the model are calculated for a surface temperature of 5°C. (b) Heat-flow anomalies in the uppermost 1000 m in response to the imposed palaeoclimatic histories. (c) Temperature anomalies in the uppermost 1000 m in response to the imposed palaeoclimatic histories. In both (a) and (b), the anomalies are calculated relative to the steady-state conditions.

hundred metres, but that in the uppermost few hundred metres temperatures will recover within a few thousand years

.

Mean annual surface temperature

When extraction of ground-source heat is considered, mean annual surface temperature is generally defined as the temperature in the ground, just below the surface, as opposed to the mean annual air temperature as defined by meteorological data. Although local effects such as type of vegetation cover, seasonal snow cover, slope angle and slope orientation may lead to deviations of up to several degrees (Blackwell et al. 1980, Lewis and Wang 1998), for the purpose of this paper they are considered equal. Figure 9a shows that mean annual surface temperatures in Scandinavia vary by ca. 10°C, from just below 0°C (Tveito et al. 2000).

From Equation (4) we see that in an area without topography, internal heat production and lateral variation in thermal conductivity (i.e., 1D conditions apply) there is a one-to-one correlation between surface temperature and the temperature at a certain depth. Although, clearly oversimplified, this relationship is, nevertheless, useful for considering the effects of varying surface temperatures at various depths. For example, given a heat flow of 60 mW m^{-2} and a thermal conductivity

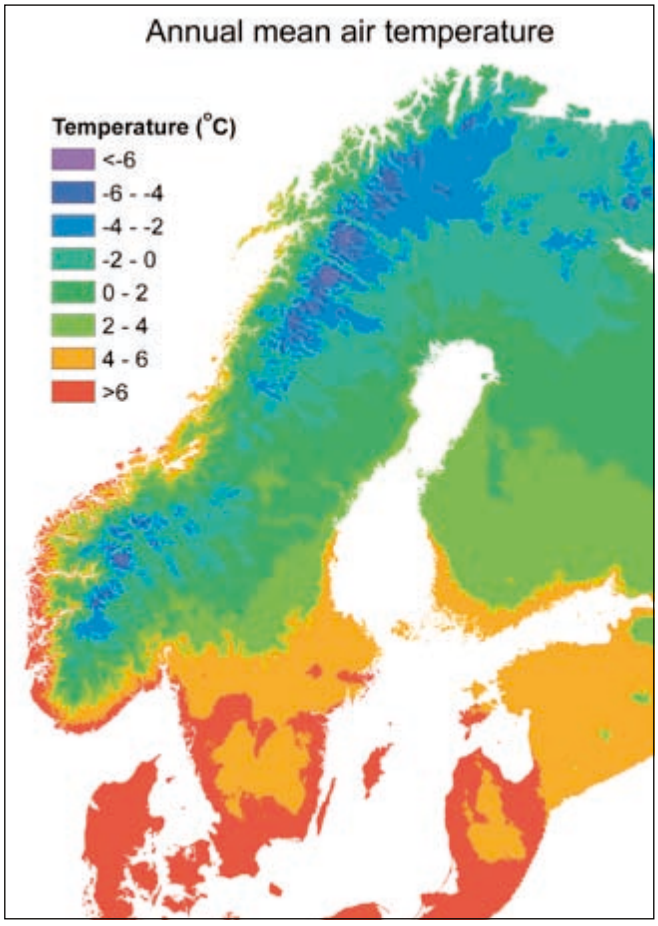

Figure 9. Mean annual air temperatures in Scandinavia. Data from the Norwegian Meteorological Institute (Tveito et al. 2000).

of 3 W m^{-1} K^{-1}, surface temperatures of 0 and 10°C result in 2/12°C at 100 m depth, 4/14°C at 200 m depth and 20/30°C at 1000 m depth. The relative temperature change at each depth resulting from this variation in surface temperature is 6-fold at 100 m depth, 3.5-fold at 200 m depth, and only 1.5-fold at 1000 m depth. Thus, as we intuitively expect, variations in surface temperature exert a major control on temperatures at 100 and 200 m, but relatively little at 1000 m depth. The effect of varying surface temperature (and other factors) on extraction of ground-source heat is discussed below.

Shallow thermal structure and significance for utilisation of ground-source heat

The results from the above modelling show that mean annual surface temperature is the main factor controlling the temperature at shallow depths down to a few hundred metres. In contrast, relatively large variation in factors such as heat production, thermal conductivity, low-conductivity overburden, topography and palaeoclimatic history cause variation in subsurface temperatures of at most a few degrees at these depths.

A misconception that is sometimes encountered is that high heat flow or radiogenic heat production are favourable because they help replenish heat extracted from the borehole. A simple exercise shows that this notion is unreasonable. If the temperature of the rocks in immediate vicinity of the borehole is reduced by 5°C as a result of heat extraction, whereas rocks 5 m away from the borehole remain unaffected, the lateral thermal gradient towards the borehole will be 1000°C km^{-1}. Given a thermal conductivity of 3 W m^{-1} K^{-1} this equates to a heat flow of 3000 mW m^{-2}, i.e., two orders of magnitude greater than the heat flow from the Earth's interior. Figure 10 shows the increase in temperature as a function of time at the basal surface as well as 50 and 100 m above the basal surface in a cubic thermal model with sides of 200 m. The heat flow is 50 mW m^{-2} across the basal surface and all other surfaces are thermally insulating. Even after 50 years, the temperature increases are < 1°C; thus, over the life span of a ground-source heat facility or plant, terrestrial heat flow has a negligible effect. In practice, replenishment of heat takes place solely by lateral heat flow from the surrounding rock volume, whereas elevated, but nevertheless relatively miniscule, heat flow from the Earth's interior only serves to increase the ambient temperature.

Figure 11 shows the results of three models that calculate the energy output from boreholes of 100, 200 and 1000 m depth for different thermal conductivities, surface temperatures and heat flows. The model setup is shown in Figure 11a and consists of a 14 cm-diameter, water-filled borehole with a 5 cm-diameter, U-shaped collector pipe through which water, with an initial temperature of 0°C, is circulated at a rate of 0.8 l s^{-1}. Five cycles, each consisting of a 150-day circulation period followed by a 200-day recovery period with no circulation, are modelled. For each model, the net energy output is calculated at the outlet.

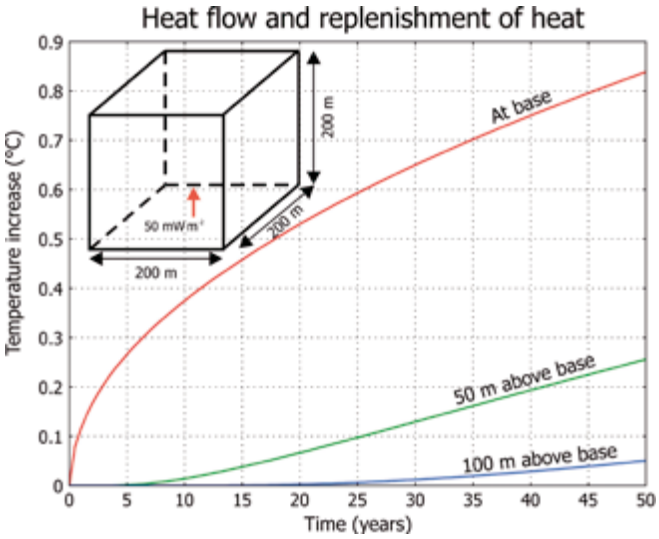

Figure 10. Cubic thermal model with sides of 200 m, thermal conductivity 3 W m^{-1} K^{-1}, heat capacity of 850 J kg^{-1} K^{-1} and density of 2800 kg m^{-3}. The heat flux is 50 mW m^{-2} across the basal surface; all other surfaces are thermally insulating. The model is shown schematically in the inset figure. The plot shows temperature increase vs. time at 0, 50 and 100 m above the basal surface.

The main point of the modelling is to determine the effect of the factors discussed above on the amount of ground-source heat extractable from boreholes of a certain depth. The results are therefore plotted in lognormal time vs. effect diagrams, and only the magnitude variation is discussed rather than the absolute energy output.

Figures 11b, c show the results of varying thermal conductivity and heat flow, respectively. The heat-flow variation, in addition to heat flow from the Earth's interior, may also be taken to represent variation in heat production, topography and climatic variation. The figures show that the amount of heat extractable from shallow to deep boreholes depends mainly on depth and relatively little on thermal conductivity and heat flow. The effects of these parameters increase with increasing depth; e.g., varying the heat flow by a factor of 2, from 40 to 80 mW m^{-2}, has a negligible effect at 100 m depth, but increases the amount of extracted heat by a factor of ca. 1.5 at 1000 m depth. Figure 11d shows the results of varying the mean annual surface temperature from 0 to 10°C. It is immediately clear from the figure that varying the surface temperature has a profound effect on the amount of heat extractable at shallow depths (100 and 200 m), whereas the effect at 1000 m is significantly smaller and comparable to varying the thermal conductivity and heat flow.

This result shows that the heat extracted from boreholes only a few hundred metres deep is mainly derived from the surface, and that geological variation is relatively insignificant. It should be noted, however, that this conclusion is valid for long-term, low-load extraction of heat. If one were to extract heat at a significantly higher rate, thus lowering the temperature around the borehole to close to the temperature of the circulating fluid, the initial temperature would be relatively insignificant and thermal conductivity would be the limiting factor. The significance of various parameters is, therefore, highly model

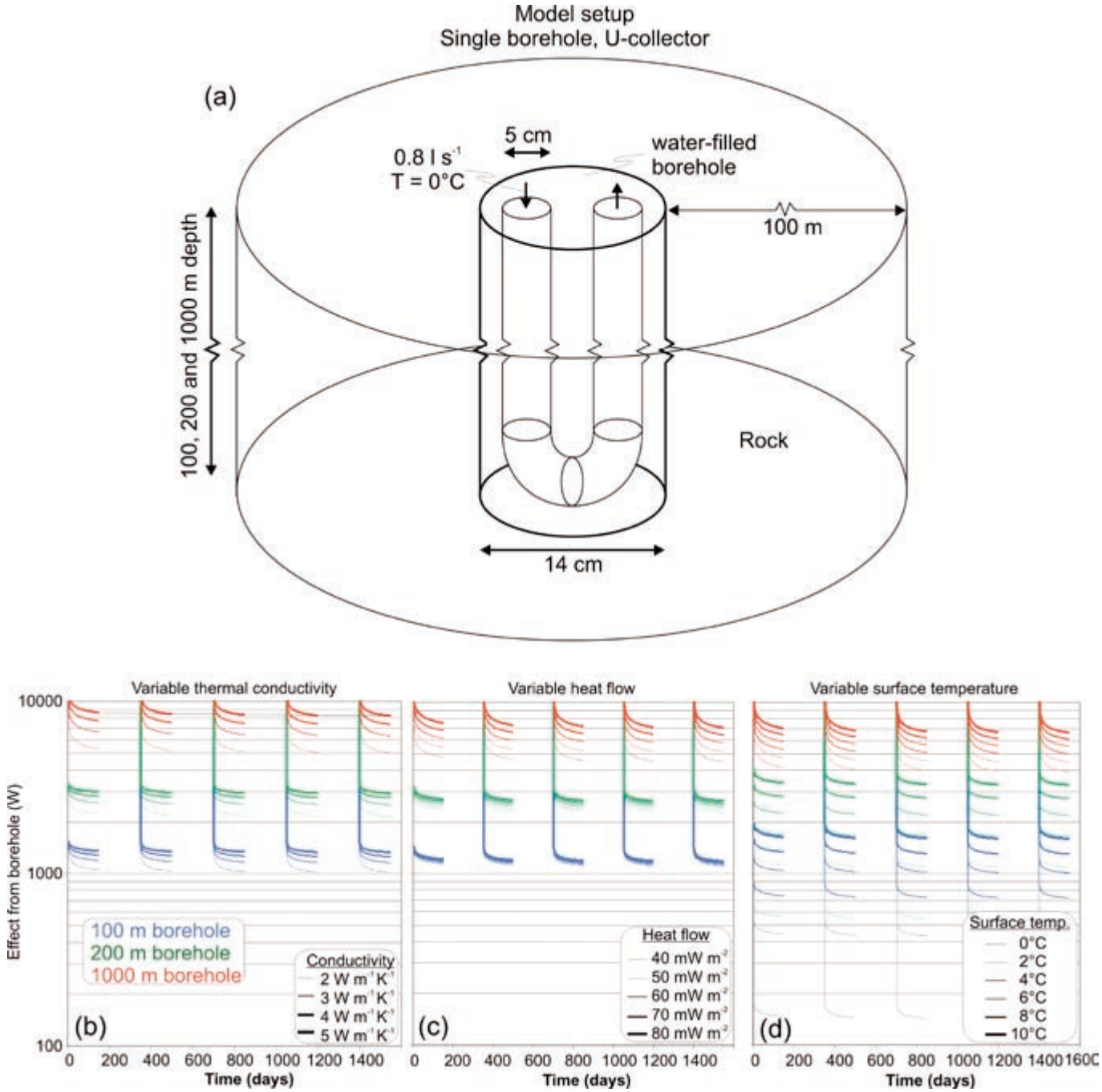

Figure 11. (a) Model setup used to determine the influence of thermal conductivity, heat flow and mean annual surface temperature on the amount of heat extractable from a borehole. The diagrams show the effects of varying (b) thermal conductivity, (c) heat flow and (d) surface temperature on the amount of heat extractable from boreholes of 100, 200 and 1000 m depth.

dependent. Other geological factors not considered here, in particular groundwater flow, may also be a significant factor locally.

Conclusions

At shallow crustal levels, i.e., down to a few hundred metres, mean annual surface temperature is the main controlling factor on temperature. Other factors, including heat flow, heat production, thermal conductivity, low-conductivity overburden, topography and palaeoclimatic history play relatively minor roles. At greater depths, these factors progressively come into play and ultimately dominate.

Efficient use of ground-source heat is first and foremost a question of developing cheaper drilling techniques and more efficient heat pumps and heat exchangers. Other factors,

including geological information, play rather secondary roles. However, with the advent of cheaper, more efficient drilling techniques allowing deeper boreholes at an affordable price, geological knowledge will be highly valuable.

Acknowledgements

Christophe Pascal and Jan Steinar Rønning are thanked for critical comments that improved the paper. The work was supported by NGU project 277100, 'Efficient use of ground-source heat'.

References

Anderson, E.M. (1934) Earth contraction and mountain building. *Beitrage zur Geophysik*, **42**, 133–159.

Benfield, A.E. (1939) Terrestrial heat flow in Great Britain. *Proceedings of the Royal Society of London, Series A*, **173**, 474–502.

Blackwell, D.D., Steele, J.L. and Brott, C.A. (1980) The terrain effect on terrestrial heat flow. *Journal of Geophysical Research*, **85**, 4757–4772.

Clauser, C. and Huenges, E. (1995) Thermal conductivity of rocks and minerals. *Rock Physics and Phase Relations. A Handbook of Physical Constants. AGU Reference Shelf 3*, pp. 105–126.

Clauser, C., Giese, P., Huenges, E., Kohl, T., Lehmann, H., Rybach, L., Šfanda, J., Wilhelm, H., Windloff, K. and Zoth, G. (1997) The thermal regime of the crystalline continental crust: Implications from the KTB. *Journal of Geophysical Research*, **102**, 18417–18441.

Grønlie, G., Heier, K.S. and Swanberg, C.A. (1977) Terrestrial heat-flow determinations from Norway. *Norsk Geologisk Tidsskrift*, **57**, 153–162.

Heier, K.S. and Grønlie, G. (1977) Heat flow–heat generation studies in Norway. *In* Saxena, S.K. and Bhattacharji, S. (eds.) *Energetics of Geological Processes*, Springer Verlag, New York, pp. 217–235.

Hofmeister, A.M. and Criss, R.E. (2005) Earth's heat flux revised and linked to chemistry. *Tectonophysics*, **395**, 159–177.

Landström, O., Larson, S.Å., Lind, G. and Malmqvist, D. (1980) Geothermal investigations in the Bohus granite area in southwestern Sweden. *Tectonophysics*, **64**, 131–162.

Lewis, T.J. and Wang, K. (1998) Geothermal evidence for deforestation induced warming: Implications for the climatic impact of land development. *Geophysical Research Letters*, **25**, 535–538.

Lind, G. (1982) *Gravity interpretation of the crust in south-western Sweden*. Ph.D. thesis, University of Göteborg/Chalmers University of Technology, Göteborg, 93 pp.

Midttømme, K. (1997) *Thermal conductivity of sedimentary rocks-selected methodological, mineralogical and textural studies*. Ph.D. thesis, Norwegian University of Science and Technology, Trondheim, 146 pp.

Ramberg, I. and Smithson, S. (1973) Geophysical interpretation of crustal structure along the southeastern coast of Norway and Skagerrak. *Geological Society of America Bulletin*, **86**, 769–774.

Slagstad, T. (2006) Did hot, high heat-producing granites determine the location of the Oslo Rift? *Tectonophysics*, **412**, 105–119.

Slagstad, T. (in press) Radiogenic heat production of Archaean to Permian geological provinces in Norway. *Norwegian Journal of Geology*.

Taniguchi, M. and Uemura, T. (2005) Effects of urbanization and groundwater flow on the subsurface temperature in Osaka, Japan. *Physics of the Earth and Planetary Interiors*, **152**, 305–313.

Tveito, O.E., Førland, E., Heino, R., Hanssen-Bauer, I., Alexandersson, H., Dahlström, B., Drebs, A., Kern-Hansen, C., Jónsson, T., Vaarby Laursen, E. and Westman, Y. (2000) Nordic temperature maps. *DNMI-Report 09/00 KLIMA*, 54 pp.